Ab Initio Comparison of the $(MX_2)_2$ Dimers (M = Zn, Cd, Hg; X = F, Cl, H) and Study of Relativistic Effects in Crystalline HgF_2

Martin Kaupp* and Hans Georg von Schnering

Max-Planck-Institut für Festkörperforschung, Heisenbergstrasse 1, 70569 Stuttgart, Germany

Received March 18, 1994[⊗]

Structures and binding energies of the dimers $(MX_2)_2$ (M = Zn, Cd; X = F, Cl, H) have been computed at the ab initio pseudopotential MP2 and HF levels and compared to recent theoretical data for the corresponding mercury species. Except for Cd_2H_4, all ZnX_2 and CdX_2 dimers exhibit symmetrically bridged D_{2h} structures. This agrees with nonrelativistic but not with quasirelativistic pseudopotential calculations for $(HgHal_2)_2$ as the latter predict loose C_{2h} complexes of almost linear monomers. Thus, relativistic effects are responsible for the discontinuities in the structural preferences down group 12. Similarly, the relativistic reduction of the HgX_2 dimerization energies changes the trends in the dimerization energies from Hg > Cd > Zn to Cd > Zn ≫ Hg. Periodic Hartree-Fock calculations on crystalline MF_2 (M = Cd, Hg) with quasirelativistic and nonrelativistic pseudopotentials confirm that relativistic effects influence the bulk properties of HgX_2 compounds exactly as suggested by the molecular model studies. In particular, relativity reduces the sublimation energy and probably also the boiling and melting points of HgF_2 considerably, in spite of a simultaneous relativistic reduction of the lattice constant. The structural and energetic trends of group 12 compounds with electronegative elements may be understood on the basis of electrostatic bonding contributions and the reduction of these by relativity for mercury.

Introduction

Many properties of group 12 compounds show a strongly nonmonotonous behavior down the group. In particular, mercury exhibits a structural chemistry which is distinctly different from those of its lighter homologues, zinc and cadmium.[1-4] The typical coordination arrangements for Zn and Cd compounds are regular tetrahedral and octahedral, respectively.[1-3] In contrast, mercury frequently features linear two-coordination with electronegative substituents, supplemented by additional weaker contacts.[1,2,4] Moreover, zinc and particularly cadmium compounds with electronegative elements often exhibit relatively high melting and boiling points consistent with considerable ionic character (cf., e.g. Table 1). In contrast, the corresponding mercury species melt and boil at lower temperatures, suggesting a more covalent character and reduced intermolecular interactions for these compounds (Table 1). Obviously, the discontinuities in the aggregation behavior of group 12 compounds will also be important in understanding reactivity trends down the group.

In a recent computational study of the HgX_2 dimers (X = Hal, H),[5] we have shown that relativistic effects strongly reduce the interactions between monomeric HgX_2 molecules (by ca. 60-70%). As a consequence, the dimers are loose C_{2h} complexes of almost linear HgX_2 monomers, whereas nonrelativistic calculations would suggest symmetrically bridged D_{2h} structures (except for X = H).[5] These structural and energetic effects of relativity have been found to be related to a reduction of electrostatic bonding contributions.[5] We now provide the corresponding data for the $(ZnX_2)_2$ and $(CdX_2)_2$ dimers (X = F, Cl, H). This allows a comparison of the aggregation behavior encompassing compounds of all group 12 elements. In particular, the structures of the dimers (do they prefer symmetrically bridged D_{2h} or unsymmetrically bridged C_{2h} arrangements?), as well as the dimerization energies and their correlation with melting and boiling points of the bulk MX_2 compounds, are of interest. Experimental data for the dimers are restricted to some IR frequencies for the mercury species, which we discussed previously.[5] No structural or vibrational data for the lighter group 12 MX_2 dimers are available, even though Zn_2Cl_4 has been found by mass spectrometry.[6]

As an important extension to our molecular model studies, we need to show that the conclusions drawn from these may indeed be transferred to the solid-state aggregation behavior. Therefore we evaluate the influence of relativistic effects on the structure and sublimation energy of crystalline HgF_2 by periodic Hartree-Fock calculations with quasirelativistic and

Table 1. Melting (Boiling) Points (°C) of the Group 12 Dihalides MX_2[a]

	M		
X	Zn	Cd	Hg
F	872 (ca. 1500)	1110 (1747)	645 dec (647)
Cl	275 (756)	568 (980)	277 (304)
Br	394 (697)	568 (1136)	241 (319)
I	446 (decs. 625)	387 (790)	257 (354)

[a] Data from ref 2.

* Author to whom correspondence should be addressed.

[⊗] Abstract published in *Advance ACS Abstracts,* September 1, 1994.

(1) (a) Cotton, F. A.; Wilkinson, G. *Advanced Inorganic Chemistry,* 5th ed.; Wiley: New York, 1988. (b) Greenwood, N. N.; Earnshaw, A. *Chemistry of the Elements*; Pergamon Press: Oxford, England, 1984. (c) Wells, A. F. *Structural Inorganic Chemistry,* 5th ed., Clarendon Press: Oxford, England, 1984.

(2) Aylett, B. J. In *Comprehensive Inorganic Chemistry*; Trotman-Dickenson, A. F., Ed.; Pergamon Press: Oxford, England, 1973; Vol. 3.

(3) Prince, R. H. in *Comprehensive Coordination Chemistry*; Wilkinson, G., Ed.; Pergamon Press: Oxford, England, 1987; Vol. 5 (Zn, Cd).

(4) (a) Brodersen, K.; Hummel, H.-U. In *Comprehensive Coordination Chemistry*; Wilkinson, G., Ed.; Pergamon Press: Oxford, England, 1987; Vol. 5 (Hg). (b) Grdenic, D. *Q. Rev. Chem. Soc.* **1965,** *19,* 303. (c) Dean, P. A. W. *Prog. Inorg. Chem.* **1978,** *24,* 109. (d) Grdenic, D. In *Structural Studies of Molecular Biological Interest*; Dodson, G., Glusker, J. P., Sayre, D., Eds.; Clarendon Press: Oxford, England, 1981. (e) Levason, W.; McAuliffe, C. A. In *The Chemistry of Mercury*; McAuliffe, C. A., Ed., Macmillan: London, 1977.

(5) Kaupp, M.; von Schnering, H. G. *Inorg. Chem.* **1994,** *33,* 2555.

(6) Bulanov, A. D.; Verkoturov, E. N.; Makarov, A. V.; Pronchetov, A. N. *Vysokochist. Veskchestva* **1991,** 5.

0020-1669/94/1333-4718$04.50/0

nonrelativistic pseudopotentials, and compare the results to those for CdF_2 and to experiment.

Computational Methods

A. Molecular Calculations. The MX_2 monomers were optimized in $D_{\infty h}$ symmetry at the Hartree–Fock (HF) and MP2 levels of ab initio theory.[7] The structures of the dimers $(MX_2)_2$ have been computed within C_{2h} symmetry at HF. In all cases, except for $(CdH_2)_2$ (and for the mercury species[5]), the HF optimization converged to a symmetrically bridged D_{2h} structure. The subsequent MP2 optimizations were restricted to D_{2h} symmetry. For $(CdH_2)_2$, both the D_{2h} transition state and the C_{2h} minimum have been optimized at the HF and MP2 levels.

We employed the same quasirelativistic energy-adjusted metal 20-valence-electron pseudopotentials and (8s7p6d)/[6s5p3d] valence basis sets[8,9] used in our recent computational studies on group 12 chemistry.[5,10] For the halogen atoms, we used quasirelativistic 7-valence-electron pseudopotentials[11a] and (5s5p1d)/[3s3p1d] valence basis sets including diffuse functions.[11b,c] A (4s1p)/[2s1p] basis was employed for hydrogen.[12] More accurate single-point calculations for the MX_2 monomers at the MP2 and quadratic configuration interaction (QCISD and QCISD(T))[13] levels were carried out with flexible, generally contracted ANO[14] valence basis sets of the sizes (8s7p6d2f)/[4s3p3d2f] for Zn, Cd, and Hg,[10] (7s7p3d1f)/[3s3p3d1f] for F and Cl,[10] and (7s2p)/[3s2p] for H.[15]

The MP2 and QCI calculations correlated all electrons available outside the pseudopotential cores, including the metal $(n-1)$ shell. Contributions from basis set superposition errors (BSSE) to the MP2 dimerization energies have been estimated by the counterpoise procedure.[16] The molecular calculations have been carried out with the Gaussian 92[17] and MOLPRO[18] program packages.

B. Periodic Hartree–Fock Calculations. Our periodic Hartree–Fock calculations on bulk HgF_2 and CdF_2, with the Crystal 92 program,[19] used the same quasirelativistic and nonrelativistic Hg pseudopotentials and quasirelativistic Cd pseudopotential[9] as our molecular calculations. Due to program limitations, the f-projectors of the pseudopotentials had to be employed as local terms and were subtracted from the s-, p-, and d-projectors. Molecular test calculations showed a negligible effect of this modification. The fluorine pseudopotential could be used unaltered. The most diffuse p- and d-function, the two most diffuse s-functions of the abovementioned segmented metal basis sets, and the diffuse sp- and polarization d-functions of the segmented fluorine basis were deleted. The exponent of the most diffuse d-function in the resulting 4s4p2d metal basis set was increased to 0.250 for Hg and to 0.260 for Cd.

It appears reasonable to assume that the fluorite structure known experimentally for HgF_2[20] will also be the most stable structure at the nonrelativistic level. This electrostatically most favorable arrangement is also found for CdF_2.[21] Thus, only the unique lattice constants a of the *Fm3m* structures have been optimized by pointwise variation and a quadratic fit. For HgF_2, both the quasirelativistic and the nonrelativistic Hg pseudopotential[9] have been used. The overlap and penetration thresholds for the calculation of the Coulomb and exchange integrals (ITOL1–ITOL5 in the Crystal92 program[19]) have been set to 10^{-5}, 10^{-5}, 10^{-5}, 10^{-6}, and 10^{-12}, respectively. SCF convergence criteria of 10^{-6} au for energies and densities have been used. The counterpoise correction[16] (involving only nearest-neighbor basis functions for the crystal) was used to estimate and correct for BSSE in the calculated lattice, atomization, and sublimation energies.

Table 2. MP2 and HF Optimized and Experimental Bond Distances (Å) in Group 12 MX_2 Monomers

M	X	MP2[a]	HF[a]	exptl[b]
Zn	F	1.741	1.743	1.742(2)
Zn	Cl	2.089	2.116	2.062(4)
Zn	H	1.509	1.558	
Cd	F	1.959	1.949	
Cd	Cl	2.292	2.314	
Cd	H	1.672	1.708	
Hg[c]	F	1.965	1.953	
Hg[c]	Cl	2.293	2.313	2.252(5)
Hg[c]	H	1.632	1.664	

[a] Segmented basis. [b] Experimental data taken from: Hargittai, M. *Coord. Chem. Rev.* **1988**, *94*, 78. [c] Cf. ref 5.

Structures and Atomization Energies of the MX_2 Monomers

Table 2 summarizes the M–X bond distances for the MX_2 monomers at the same theoretical levels used below for the dimers. The few available experimental data are also included. As expected,[5] the bond contraction due to electron correlation increases with decreasing electronegativity of the ligand. Due to the limited basis sets, our MP2 distances for X = Cl are still slightly too large. Due to some cancellation of basis set errors and errors inherent to the MP2 method, the MP2 value for HgH_2 is in good agreement with more elaborate calculations.[22]

Comparison of the MP2 atomization energies to those at higher theoretical levels (cf. Table 3) provides a particularly stringent test for the accuracy of our calculations. Data for M = Hg[5] have been included for comparison. The segmented-basis MP2 results are slightly (ca. 15–35 kJ mol^{-1}) above the ANO–MP2 values (except for M = Zn), probably partially due to basis set superposition errors, and due to the slight bias of the ANO basis sets toward the atoms.[10] However, the overall agreement is quite satisfactory. Thus, we may expect the smaller basis sets to provide reasonable dimer structures and dimerization energies (cf. below). For X = H, ANO–MP2 slightly underestimates the ANO-QCI atomization energies (by

(7) Explanations of standard levels of ab initio MO theory, such as the Hartree–Fock (HF) and MPn methods, may be found, e.g., in: Hehre, W. J.; Radom, L.; Schleyer, P. v. R.; Pople, J. A. *Ab Initio Molecular Orbital Theory*, Wiley: New York, 1986.
(8) Dolg, M.; Wedig, U.; Stoll, H.; Preuss, H. *J. Chem. Phys.* **1987**, *86*, 866.
(9) Andrae, D.; Häussermann, U.; Dolg, M.; Stoll, H.; Preuss, H. *Theor. Chim. Acta* **1990**, *77*, 123.
(10) (a) Kaupp, M.; von Schnering, H. G. *Angew. Chem.* **1993**, *105*, 952. Kaupp, M.; von Schnering, H. G. *Angew. Chem., Int. Ed. Engl.* **1993**, *32*, 861. (b) Kaupp, M.; Dolg, M.; Stoll, H.; von Schnering, H. G. *Inorg. Chem.* **1994**, *33*, 2122.
(11) (a) Bergner, A.; Dolg, M.; Küchle, W.; Stoll, H.; Preuss, H. *Mol. Phys.* **1993**, *80*, 1431. (b) Kaupp, M.; Schleyer, P. v. R.; Stoll, H.; Preuss, H. *J. Am. Chem. Soc.* **1991**, *113*, 6012. (c) Huzinaga, S., Ed. *Gaussian Basis Sets for Molecular Calculations*; Elsevier: New York, 1984.
(12) Dunning, T. H.; Hay, P. J. In *Methods of Electronic Structure Theory, Modern Theoretical Chemistry*; Schaefer III, H. F., Ed.; Plenum Press: New York, 1977; Vol. 3.
(13) See, e.g.: Pople, J. A.; Head-Gordon, M.; Raghavachari, K. *J. Chem. Phys.* **1987**, *87*, 5968. Paldus, J.; Cizek, J.; Jeziorski, B. *J. Chem. Phys.* **1989**, *90*, 4356; **1990**, *93*, 1485. Raghavachari, K.; Head-Gordon, M.; Pople, J. A. *J. Chem. Phys.* **1990**, *93*, 1486.
(14) For atomic natural orbital (ANO) basis sets, cf.: Almlöf, J.; Taylor, P. R. *J. Chem. Phys.* **1987**, *86*, 4070.
(15) Dunning, T. H. *J. Chem. Phys.* **1989**, *90*, 1007.
(16) Boys, S. F.; Bernardi, F. *Mol. Phys.* **1970**, *19*, 553.
(17) Frisch, M. J.; Trucks, G. W.; Head-Gordon, M.; Gill, P. M. W.; Wong, M. W.; Foresman, J. B.; Johnson, B. G.; Schlegel, H. B.; Robb, M. A.; Replogle, E. S.; Gomperts, R.; Andres, J. L.; Raghavachari, K.; Binkley, J. S.; Gonzalez, C.; Martin, R. L.; Fox, D. I.; DeFrees, D. J.; Baker, J.; Stewart, J. P.; Pople, J. A. Gaussian 92, Revision A. Gaussian, Inc., Pittsburgh PA, 1992.
(18) Program system MOLPRO written by: Werner, H. J.; Knowles, P. J. Contributions by: Almlöf, J.; Amos, R.; Elbert, S.; Hampel, C.; Meyer, W.; Peterson, K.; Pitzer, R.; Stone, A.
(19) Crystal 92 program by: Dovesi, R.; Saunders, V. R.; Roetti, C.; et al., 1992. For a general description, cf: Pisani, C.; Dovesi, R.; Roetti, C. *Hartree-Fock ab Initio Treatment of Crystalline Systems, Lecture Notes in Chemistry*; Springer: Berlin, 1988.
(20) Ebert, F.; Woitinek, H. *Z. Allg. Anorg. Chem.* **1933**, *210*, 269.
(21) (a) Hund, F.; Lieck, K. *Z. Allg. Anorg. Chem.* **1952**, *271*, 17. (b) Haendler, H. M.; Bernard, W. J. *J. Am. Chem. Soc.* **1951**, *73*, 5218.
(22) Schwerdtfeger, P.; Boyd, P. D. W.; Brienne, S.; McFeaters, J.; Dolg, M.; Liao, M.-S.; Schwarz, W. H. E. *Inorg. Chim. Acta* **1993**, *213*, 233.

Table 3. Comparison of Atomization Energies (kJ mol^{-1}) of the MX_2 Monomers at Different Computational Levels[a]

M	X	MP2[b]	ANO–MP2[c]	ANO–QCISD[c]	ANO–QCISD(T)[c]
Zn	F	789.5	815.7	736.9	749.1
Cd	F	699.6	677.5	621.3	636.3
Hg	F	529.7 (706.0)[d]	510.6 (680.2)[d]	460.2 (623.0)[d]	481.2 (638.2)[d]
Zn	Cl	625.2	627.0	567.2	579.9
Cd	Cl	571.3	536.9	494.8	510.2
Hg	Cl	434.9 (578.5)[d]	403.6 (542.3)[d]	366.5 (502.5)[d]	385.9 (517.6)[d]
Zn	H	409.2	410.3	419.7	418.1
Cd	H	361.9	346.1	374.5	374.9
Hg	H	344.8 (351.2)[d]	321.0 (330.4)[d]	350.0 (362.3)[d]	351.6 (362.3)[d]

[a] Based on MP2 structures obtained with the segmented valence basis sets. Note that similar data have already been reported for some of the species (cf. refs 5 and 10). [b] Segmented basis. [c] Extended ANO valence basis sets. [d] Quasirelativistic Hg pseudopotential results with nonrelativistic results in parentheses (cf. ref 5).

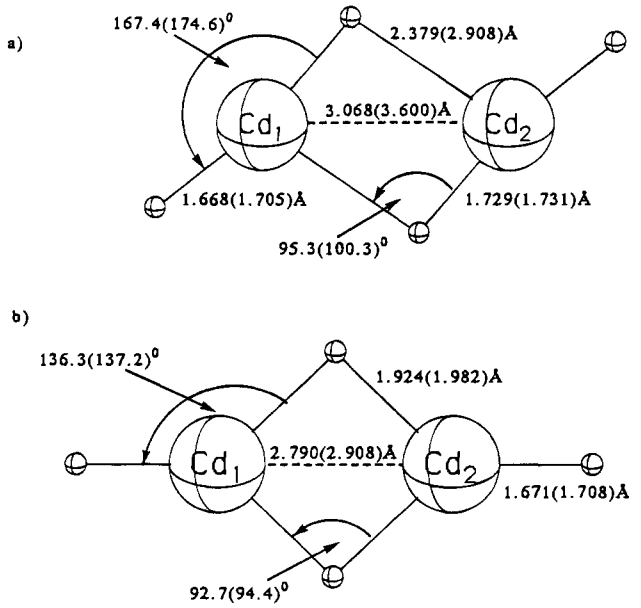

Figure 1. MP2(HF) optimized structure for Cd_2H_4: (a) C_{2h} minimum; (b) D_{2h} transition state.

ca. 10–30 kJ mol^{-1}). In contrast, MP2 considerably overestimates the electron correlation contributions for the halides (by ca. 50–80 kJ mol^{-1} compared to QCISD[10]). Contributions from connected triple excitations (i.e. QCISD(T) vs. QCISD results) have only a minor effect. Thus, while the general trends are reproduced reasonably well at MP2, an accurate absolute determination of reaction energies involving homolytic bond cleavage will require QCISD or similar theoretical levels (however, note that the QCI atomization energies given probably are in turn slightly too low due to basis set incompleteness[5]). This is consistent with calculations for similar systems.[5,10,22]

Structures of the Dimers

Table 4 summarizes the MP2(HF) optimized structures for the D_{2h} MX_2 dimers. Figure 1 shows both the D_{2h} transition structure and the C_{2h} minimum for Cd_2H_4. Notably, except for the cadmium hydride dimer, all Zn and Cd species prefer symmetrically bridged D_{2h} structures. In contrast, the HgX_2 dimers (X = Hal, H) feature very unsymmetrically bridged C_{2h} complexes at the quasirelativistic pseudopotential level.[5] As all HgX_2 dimers, except for the hydride, have D_{2h} minima in nonrelativistic calculations,[5] the structural differences between the Hg compounds and the lighter homologues are obviously due to the influence of the relativistic kinematics of electrons approaching a heavy (high-Z) nucleus like mercury.[23]

Consistent with nonrelativistic results for $(HgH_2)_2$,[5] $(CdH_2)_2$ (cf. Figure 1a) shows an intermediate behavior between the D_{2h} structures obtained for the other Zn and Cd species (Table 4) and the complexes of almost linear monomers calculated for the $(HgX_2)_2$ dimers at the quasirelativistic pseudopotential level.[5] The two bridging Cd–H distances are considerably different (by ca. 0.65 Å at MP2), and the deviation of the H_tCdH_b angle from linearity is moderate (ca. 12° at MP2). Note the large influence of electron correlation on the structure of the complex. The HF calculations would predict an extremely loose arrangement with more linear CdH_2 fragments. The D_{2h} transition state (cf. Figure 1b) connecting two C_{2h} minima of Cd_2H_4 is only 4.8(14.0) kJ mol$^-$ above the minima at the MP2(HF) level. This is much more similar to nonrelativistic (2.0(3.5) kJ mol^{-1}) than to quasirelativistic data (95.5(121.4) kJ mol^{-1}) computed for Hg_2H_4.[5]

As expected, all bridging $M–X_b$ distances are longer than the corresponding terminal $M–X_t$ distances (Table 4). The $M–X_b–M$ angles follow the order F > H > Cl and Cd > Zn, consistent with anion and cation size considerations, and with the known hybridization trends for the halogens.

No structural data on the dimeric systems are available in the literature which could be used for direct comparison. We have previously compared experimental and calculated vibrational frequencies for the mercury species, and found reasonable agreement.[5] The closest structural analogy to the present results probably is given by the very recent X-ray structure analyses of the dimeric organometal chlorides $(RMCl)_2$ (R = $(Me_2PhSi)_3C$; M = Zn, Cd, Hg).[24] Remarkably, the zinc and cadmium compounds feature almost symmetrically chloride-bridged structures, whereas the mercury system is composed of weakly associated, almost linear monomeric units. Table 5 compares the bridging M–Cl distances in these organometallic dimers to the calculated MP2 values for the dichloride dimers. The agreement is excellent.

Dimerization Energies

The MP2(HF) dimerization energies are listed in Table 6, together with counterpoise corrected MP2 values ($MP2_{cc}$). Nonrelativistic and quasirelativistic pseudopotential results for M = Hg[5] are included for comparison. In agreement with the results for mercury, the electron correlation contributions generally reduce the dimerization energies somewhat for X = F (the largest reduction is found for ZnF_2, ca. 35 kJ mol^{-1}), but increase them for X = Cl and H. This has been rationalized by larger contributions from dispersion type interactions for the heavier halogens (the increase of the HgX_2 dimerization energies by correlation was found to be largest for X = I[5]) and also for the electron deficient hydride bridge. For related gold dimers $(XAuPH_3)_2$, the correlation contributions to the intermolecular interactions also increase with increasing softness of the ligands X.[25] However, in contrast to these gold species, "metallophilic" attractions are certainly less likely in the present case. The metal charges are considerably higher, and the d-orbitals are already much more corelike for the group 12 elements. Moreover, the bonding for the $(MX_2)_2$ dimers is dominated by dipole–dipole interactions,[5] whereas the model systems chosen in ref 25 feature an unfavorable alignment of the bond dipoles.

As estimated by the counterpoise correction,[16] BSSE contributions to the dimerization energies at MP2 range from ca. 5

(23) For a recent review of relativistic effects in heavy element chemistry, cf. e.g.: Pyykkö, P. *Chem. Rev.* **1988**, *88*, 563.
(24) Al-Juaid, S. S.; Eaborn, C.; Habtemariam, A.; Hitchcock, P. B.; Smith, J. D.; Tavakkoli, K.; Webb, A. D. *J. Organomet. Chem.* **1993**, *462*, 45.
(25) Pyykkö, P.; Li, J.; Runeberg, N. *Chem. Phys. Lett.* **1994**, *218*, 133.

Table 4. MP2(HF) Optimized Structures (D_{2h})[a] for the $(MX_2)_2$ Dimers (M = Zn, Cd; X = F, Cl, H)

species	M—X_t	MX_b	M···M	X_tMX_b	MX_bM
Zn_2F_4	1.763 (1.760)	1.937 (1.930)	2.968 (2.982)	140.0 (140.6)	100.0 (101.2)
Cd_2F_4	1.977 (1.968)	2.146 (2.140)	3.393 (3.419)	141.2 (143.1)	104.5 (106.0)
Zn_2Cl_4	2.111 (2.136)	2.305 (2.340)	3.159 (3.240)	133.3 (133.5)	86.5 (87.7)
Cd_2Cl_4	2.317 (2.337)	2.517 (2.556)	3.602 (3.686)	135.7 (135.7)	91.4 (92.4)
Zn_2H_4	1.507 (1.554)	1.727 (1.796)	2.438 (2.554)	134.9 (134.8)	89.9 (91.2)
Cd_2H_4[b]	1.671 (1.708)	1.924 (1.982)	2.790 (2.908)	136.3 (137.2)	92.7 (94.4)

[a] Optimizations in C_{2h} symmetry converged to these symmetrically bridged D_{2h} structures except for Cd_2H_4. Distances in Å; angles in deg. X_t = terminal substituent; X_b bridging substituent. [b] Transition state, cf. Figure 1b. Figure 1a for the C_{2h} minimum.

Table 5. Comparison of Bridging M—Cl Distances (Å) in the Solid-State Structures of Dimeric $(RMCl)_2$ (R = $(Ph_2MeSi)_3C$) to the MP2(HF) Optimized Values for $(MCl_2)_2$

	Zn	Cd	Hg
$(RMCl)_2$[a]			
short[b]	2.303 (2.304)	2.499 (2.515)	2.326 (2.317)
long[b]	2.335 (2.365)	2.558 (2.557)	3.194 (3.392)
$(MCl_2)_2$ MP2(HF)			
short[b]	2.305 (2.340)[c]	2.517 (2.556)[c]	2.295 (2.315)[d]
long[b]			3.130 (3.314)[d]

[a] Cf. ref 24. Data for two independent molecules in the unit cell are given; values for the second are in parentheses. [b] Shorter and longer bonds for unsymmetrical bridges. [c] Symmetrical bridge, cf. Table 4. [d] Cf. ref 5.

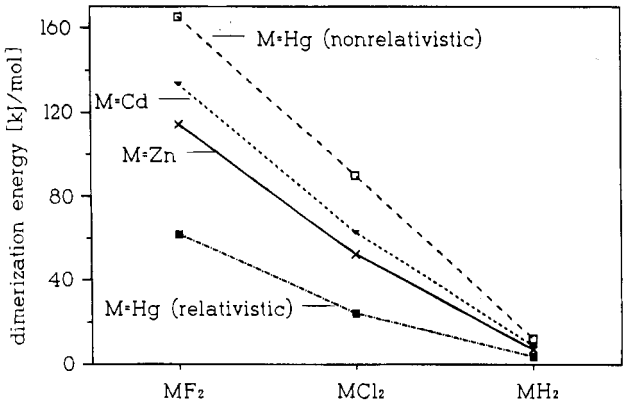

Figure 2. MP2 MX_2 dimerization energies (cf. Table 6).

kJ mol^{-1} for $(HgH_2)_2$ to ca. 34.2 kJ mol^{-1} for $(CdF_2)_2$ (cf. Table 6). Obviously, the errors are largest on an absolute scale for the more compact D_{2h} systems but smaller for the weakly bound $(HgH_2)_2$ complex. The BSSE contributions are significant compared to the absolute dimerization energies, particularly for the weakly bound dihydride dimers, but they affect the trends for different M or X only moderately.

The trends in the MP2 dimerization energies (counterpoise corrected values) are shown in Figure 2. As expected, the ordering for a given metal is F > Cl > H.[5] While the nonrelativistic results for the mercury species would predict an ordering of the dimerization energies for a given X as Hg > Cd > Zn, relativistic effects for mercury change this trend to Cd > Zn ≫ Hg. Thus, relativity is indeed largely responsible for the discontinuities, not only in the structural trends (cf. above), but also in the thermochemical trends down the group. While the uncorrected MP2(HF) values for $(ZnH_2)_2$ are somewhat larger than those for $(CdH_2)_2$ (Table 6), inclusion of counterpoise corrections leads to similar, quite small dimerization energies for the two hydrides.

Trends in Charge Separations

The structural and energetic trends discussed above may be rationalized[5] by comparing the metal charges for the MX_2 monomers (cf. Figure 3; natural population analysis, NPA,[26]

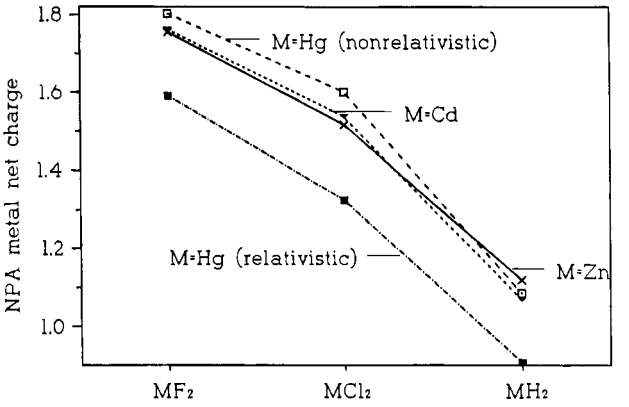

Figure 3. NPA charges for the MX_2 monomers. Hartree—Fock densities at the MP2 optimized bond lengths have been analyzed.

was employed). These show a behavior similar to that of the dimerization energies (compare Figure 2): (a) For a given M, the charges decrease with X = F > Cl > H, as expected from the electronegativities of the ligands. (b) While the charges for a given X are quite similar for M = Zn, Cd, and Hg_{nr} (i.e. the nonrelativistic values for M = Hg), the relativistic reduction of the mercury charges leads to a much smaller charge separation in the HgX_2 monomers than for the corresponding zinc and cadmium species. Taking into account the bond length variations (cf. Table 4 and ref 5), the trends in the charge separations for the monomers correlate indeed remarkably well with their aggregation behavior. Particularly for the fluorides and chlorides, this suggests large electrostatic contributions to the driving force for dimerization (cf. ref 5 for a more detailed discussion of the relativistic contributions with M = Hg, and for an evaluation of alternative explanations).

Relativistic Effects in Solid HgF_2

Table 7 shows various computed and experimental properties for crystalline HgF_2 and CdF_2. For the former, both the quasirelativistic and nonrelativistic Hg pseudopotential results are compared. Relativity contracts the lattice constant a of HgF_2 by ca. 0.07 Å, and thus the Hg—F distance by ca. 0.03 Å (from 2.434 to 2.405 Å). This contraction is less than that computed for the bridging Hg—F distances in dimeric HgF_2 (ca. 0.06 Å for the D_{2h} structure at the HF level[5]) and considerably less than that for the terminal distance in $(HgF_2)_2$[5] or the monomeric HgF_2 (ca. 0.11 Å at HF[5]). Thus, the magnitude of the relativistic bond contraction decreases with decreasing formal bond valence.[27] Following the frequently used arguments of Ziegler et al.,[28] this may be rationalized by smaller Hg 6s-orbital contributions to bonding (e.g. the NPA net Hg 6s-population in the HgF_2

(26) (a) Reed, A. E.; Weinhold, F. *J. Chem. Phys.* **1985**, *83*, 1736. (b) Reed, A. E.; Curtiss, L. A.; Weinhold, F. *Chem. Rev.* **1988**, *88*, 899.
(27) For a definition of bond valence, cf. e.g.: Pauling, L. *The Nature of the Chemical Bond*, 3rd ed.; Cornell University Press: Ithaca, NY, 1960.
(28) See, e.g.: Ziegler, T.; Snijders, J. G.; Baerends, E. J. *Chem. Phys. Lett.* **1980**, *75*, 1. Also cf. ref 23 and references cited therein.

Table 6. Comparison of MP2(HF) Dimerization Energies (kJ mol^{-1}1) for MX_2 (M = Zn, Cd, Hg; X = F, Cl, H)[a]

		F		Cl		H	
M	X	MP2(HF)	$MP2_{cc}$[b]	MP2(HF)	$MP2_{cc}$[b]	MP2(HF)	$MP2_{cc}$[b]
Zn		143.6 (177.8)	114.3	86.5 (71.6)	52.3	30.0 (15.0)	7.2
Cd		167.8 (184.6)	133.6	96.3 (79.4)	63.0	22.3 (9.1)	8.8
Hg_{nr}[a,c]		190.3 (207.6)	165.1	119.0 (104.1)	90.1	29.1 (16.3)	12.4
Hg_{rel}[a,d]		71.6 (79.9)	61.9	36.1 (18.5)	24.3	8.7 (2.0)	3.7

[a] Results for M = Hg from ref 5. [b] Counterpoise-corrected MP2 values. [c] Nonrelativistic Hg pseudopotential. [d] Quasirelativistic Hg pseudopotential.

Table 7. Calculated Atomization (ΔE_{at}), Lattice (ΔE_{lat}), and Sublimation (ΔE_{sub}) Energies (kJ mol^{-1}) as Well as Lattice Constant a (Å) and Bulk Modulus B_0 (GPa) for Crystalline HgF_2 and CdF_2

	ΔE_{at}[a]	ΔE_{lat}[a]	ΔE_{sub}[a]	a	B_0
Hg					
nr[c]	691.6 (989.7)	2627.8 (2925.9)	298.5 (476.1)	5.622	22.2
rel[b]	414.5 (690.4)	2705.1 (2981.0)	138.7 (299.3)	5.553	48.4
exptl[d]		2740.4	128.9	5.54	
Cd					
rel[b]	730.6 (1026.1)	2742.0 (3037.5)	260.2 (429.2)	5.408	43.7
exptl[d]		2769.7	234.2	5.388	

[a] Counterpoise-corrected energy values with uncorrected results in parentheses. [b] Quasirelativistic Hg pseudopotential used. [c] Nonrelativistic Hg pseudopotential used. [d] Cf. refs 2, 20, 21. Enthalpies, ΔH_0, are given.

dimer is only 0.448 compared to 0.558 in the monomer[5]). As a result, the lattice constants and bond distances in solid CdF_2 are significantly smaller than those for HgF_2 while the molecular bond distances are quite similar.[10] Note that the relativistic lattice constants are in excellent agreement with experiment, consistent with a small influence of core-valence correlation (and partly due to a compensation between correlation errors and BSSE). The bulk modulus B_0 of solid HgF_2 is relativistically more than doubled (consistent with relativistic effects on stretching force constants or frequencies in comparable molecular systems[22]), but only slightly larger than the value calculated for CdF_2.

The calculated energies of sublimation, atomization, and the lattice energy suffer severely from basis set superposition errors (BSSE), and thus the smaller counterpoise-corrected values probably are more accurate (cf. Table 7). However, BSSE does not affect the relativistic contributions for HgF_2 appreciably: Relativity reduces the energies of atomization and sublimation by more than 250 (35%) and 150 kJ mol^{-1} (50%), respectively. This should be compared to a relativistic reduction in the MP2 atomization energy of molecular HgF_2 by ca. 176 kJ mol^{-1} (ca. 25%[5,10]) and to a reduction in the MP2 dimerization energy of HgF_2 by ca. 120 kJ mol^{-1} (ca. 60%[5]), respectively. The resulting (counterpoise-corrected) atomization energy of solid HgF_2 is too low by ca. 37% compared too experiment, probably due to the neglect of electron correlation. In contrast, the sublimation energy is slightly too high. This is consistent with the fact that electron correlation actually reduces the dimerization energies of the group 12 difluorides (in contrast to the other halides, cf. Table 6). However, it should be noted that the experimental uncertainties for solid HgF_2 are relatively large, due to its high reactivity near the boiling temperature.[2]

Conclusions

Extending our previous investigations on the HgX_2 dimers[5] to the lighter homologues, Zn and Cd, the present work provides an ab initio comparison of the dimerization of dihalides and dihydrides of all group 12 elements. The results show clearly that the reduction of intermolecular interactions between the HgX_2 units by relativity is responsible for the discontinuities in the structural and energetic trends for the coordination of the group 12 metals to electronegative elements.

Periodic Hartree–Fock calculations on crystalline HgF_2, using quasirelativistic and nonrelativistic pseudopotentials, show that the relativistic reduction of aggregation energies found for the HgX_2 dimers is also transferred to the properties of the bulk material. Relativistic effects are responsible for the low sublimation energies and low boiling points of many mercury species compared to their zinc and cadmium homologues.

This has far-reaching consequences for the chemistry of mercury. A full account of the phenomena that are likely to be influenced by the relativistic increase in the electronegativity[29] of mercury is certainly beyond the scope of this paper (cf. ref 23 for the most recent relevant review). We only mention that the extensive mercury(I) (Hg_2^{2+}) chemistry, as well as the potential existence of a mercury(IV) chemistry (HgF_4?[10]), are only possible due to the relativistic destabilization, either intra- or intermolecularly, of the corresponding "regular" mercury(II) compounds.[10,30] Important reactions like mercuration or oxymercuration in organic synthesis,[31] or the process of the mercury cell,[1b] probably owe their feasability to the relativistic reduction of intra- or intermolecular interactions in compounds of mercury with electronegative elements. Similarly, the "relativistic" weakness of the Hg–O bond certainly contributes to the well-known stability[1] of organomercury compounds toward oxidation or hydrolysis. Further theoretical investigations are needed to assess the full scope of these relativistic influences on mercury chemistry.

Acknowledgment. We thank Prof. J. David Smith (University of Sussex) for a preprint of ref 24.

(29) In view of the probably small negative electron affinity of mercury, the relativistically increased (cf. ref 10) first ionization energy of mercury clearly accounts for a drastic increase in its electronegativity.
(30) Kaupp, M.; von Schnering, H. G. *Inorg. Chem.*, in press.
(31) See, e.g.: March, J. *Advanced Organic Chemistry*, 3rd ed.; Wiley: New York, 1985.